Electrochimica Acta, Vol. 32, No. 12, pp. 1743–1749, 1987.
Printed in Great Britain.

0013–4686/87 $3.00 + 0.00

ELLIPSOMETRY OF POLYCRYSTALLINE IRON ELECTRODES IN ALKALINE SOLUTIONS CONTAINING CHLORIDE IONS UNDER DIFFERENT ELECTROCHEMICAL CONDITIONS

S. JUANTO, J. O. ZERBINO, M. I. MIGUEZ*, J. R. VILCHE and A. J. ARVIA†

Instituto de Investigaciones Fisicoquímicas Teóricas y Aplicadas INIFTA, Facultad de Ciencias Exactas, Universidad Nacional de La Plata, Sucursal 4, Casilla de Correo 16, (1900) La Plata, Argentina

(*Received* 31 *March* 1987)

Abstract—The ellipsometric and voltammetric responses of iron in 0.04 M NaOH + xM NaCl ($0 \leqslant x \leqslant 0.3$) are investigated. Three main processes, barrier layer formation, outer layer formation and pitting corrosion which depend differently on the presence of NaCl can be distinguished. The first process becomes practically independent of NaCl concentration. Otherwise, under certain conditions NaCl increases the charge associated with the outer layer formation through pitting. The dependence of the latter on NaCl concentration is in agreement with data earlier reported in the literature. A relation among the three processes is discussed in terms of competitive anion adsorption on iron specimen and formation of redox couples within the hydrous oxide layer produced on iron.

INTRODUCTION

The formation of passivating layers on iron in base solution and their structure in the absence of oxygen have been the matter of many publications in the last few decades, particularly after the development of optical reflection techniques. The literature on the subject is reviewed in references[1–3]. However, despite these contributions the corrosion and passivation of iron still can not be completely handled as the number of variables involved in those processes is larger than earlier thought. The behaviour of iron in alkaline solution can be roughly described by taking into account whether aggressive anions are absent or present in the aqueous solutions.

In the absence of aggressive anions, *in-situ* Raman spectroscopy studies of iron passivation in 1 M KOH during oxidation–reduction cycles[4] were interpreted through the formation of Fe_3O_4 whereas in other cases[5, 6] the surface layer produced at 1 mV s^{-1} appeared to be composed of δ-FeOOH which by subsequent cycling is converted to Fe_3O_4. Likewise, the spectra of the outer passivation layer after prolonged potential cycling at 50 mV s^{-1} was assigned to α-FeOOH. Ellipsometric measurements of iron cycled galvanostatically in 0.05 M NaOH show that a low density FeOOH layer builds up progressively over an inner compact Fe_3O_4 barrier layer[7]. On the other hand, the electrochemical and ellipsometric transient behaviour of the anodic film growth on iron in 0.05 M NaOH at different potentials in the passive region after the electrode potential was rapidly changed at 80 V s^{-1} from a fixed potential in the HER region concluded that the passive film formed for times longer than 2 s can be identified as Fe_3O_4[8]. Otherwise, the examination of passive anodic oxides on iron in 1 M NaOH by X-ray photoelectron spectroscopy after specimen preparation and transfer in an oxygen-free closed system[9] reveals that the film potentiostatically formed consists of an inner FeO, $Fe(OH)_2$ layer and an outer Fe_2O_3 layer. The latter should be absent at sufficiently negative potentials. Most recently potential-modulated reflectance spectra of the passive film on iron in 0.1 M NaOH at different potentials after an anodic sweep at 10 mV s^{-1}[10] at high positive potentials were assigned to magnetite, hematite, or both, while the film in the initial prepassive region exhibits the presence of Fe^{2+} ion. Recent attempts to correlate ellipsometric and voltammetric results in either NaOH or $Ca(OH)_2$ solutions at the same pH led to the conclusion that the structure of the passivating layer and its properties change also appreciably with the cation in solution[3, 11].

Current transients and also optical parameters and thickness of passive films on iron in NaOH solution in the presence of NaCl at pH 12 indicate that pitting can occur only when the surface layer is not yet sufficiently consolidated[12], probably because it contains a large amount of incorporated water. At fixed concentration of NaCl both electrode potential and passive film water content contribute to passivity breakdown. The high pitting potentials of iron in NaOH solutions containing NaCl within the 10–13 pH range were interpreted as due to a chemical depassivation of the γ-Fe_2O_3 layer accompanied by the accumulation of chloride ions at the metal-solution interface[13].

These different views on fundamental aspects of the corrosion and passivation of iron in base solutions suggested the convenience of extending the previous work on the correlation of ellipsometry–voltammetry data of iron in NaOH by adding different concentrations of NaCl.

*Present address, Instituto Nacional de Tecnología Industrial (INTI), Sector Electroquímica Aplicada, Casilla de Correos 157, (1650) San Martín, Argentina.

†Author to whom correspondence should be addressed.

EXPERIMENTAL

The working electrodes consisted of circular (0.785 cm^2) high purity polycrystalline iron samples ("Specpure", Johnson Matthey Chemicals Ltd.) supported on PTFE holders. They were previously polished with 400 and 600 grade emery papers and 1.0, 0.3, and 0.05 μ grits alumina-acetone suspensions on polishing cloths (Microcloth), then thoroughly rinsed with thrice distilled water, and finally, held for 5 min at $E = -1.36$ V, that is in the potential region of net hydrogen evolution to attain a reproducible electroreduced metal surface[3, 11].

A three compartment electrolysis glass cell was employed to lodge the working electrode, reference electrode and counterelectrode. The working electrode was horizontally placed at the bottom of the main compartment, which was provided with two plane glass windows, which were adequated for ellipsometric measurements. The potential of the working electrode was measured against a reversible hydrogen electrode in the cell solution but in the text they are referred to the NHE scale. The counterelectrode was a large area spiral-shaped Pt wire.

Electrochemical and ellipsometric runs were made in 0.04 M NaOH + x M NaCl ($0 \leqslant x \leqslant 0.3$) solutions, at 25°C under N_2 gas saturation. The electrolyte solutions were prepared from a.r. (p.a. Merck) reagents and thrice distilled water previously boiled to remove CO_2.

The electrolysis cell was assembled in a Rudolph Research type 437–02/200 B manual ellipsometer (maximum resolution 0.01°) provided with a 150 W tungsten lamp with filter (5461 Å) and a RCA 1P 21 photomultiplier. The incidence light beam angle was fixed at 69° and that of the compensator at 135°. The complex refractive index of the substrate ($\bar{n}_s = n_s - ik_s$) at 5461 Å for polished iron electrode held at -1.36 V obtained from polarizer (P_0) and analyzer (A_0) readings was coincident with data previously reported in the literature[14, 15].

The ellipsometric characteristics of the working electrode surface were followed by perturbing with different potential–time programmes. Procedure A implied an electrode pretreatment with either a single (STPS) or a repetitive (RTPS) triangular potential sweep at $v = 20\ V\,s^{-1}$ between cathodic ($E_{s,c}$) and anodic ($E_{s,a}$) switching potentials suitable to produce a net anodic layer on the electrode surface. Immediately afterwards the anodic layer was held during a certain time (τ) at either $E_{s,a}$ (potentiostatic stabilization and growth) or $E_{s,c}$ (potentiostatic electroreduction). Procedure B was similar to procedure A, but after holding the potential at either $E_{s,a}$ or $E_{s,c}$ for the time τ, the current was switched off during different times τ_0, and immediately afterwards the voltammetric scan was continued on from the corresponding open circuit potential.

The ellipsometric readings (P and A) of the electrode covered with anodic products were made under either extinction condition or by following the change of P through the variation of the reflected light intensity, depending whether the time window (τ and τ_0) values of each run were greater or lower than 30 s, respectively.

For the sake of comparison, voltammograms in the $0.002 \leqslant v \leqslant 20\ V\,s^{-1}$ range were also run to follow anodic and cathodic contributions in the different potential ranges.

RESULTS

Electrochemical data

The STPS voltammograms of polycrystalline iron in 0.04 M NaOH (Fig. 1a) and 0.04 M NaOH + 0.05 M NaCl (Fig. 1b) run between about -1.26 and *ca* 0.04 V at different v show four anodic peaks (I, II, III, and III') and two cathodic peaks (IV and V). After ten potential cycles the increase in charge of peaks III and IV and the appearance of a new cathodic contribution (peak IV')

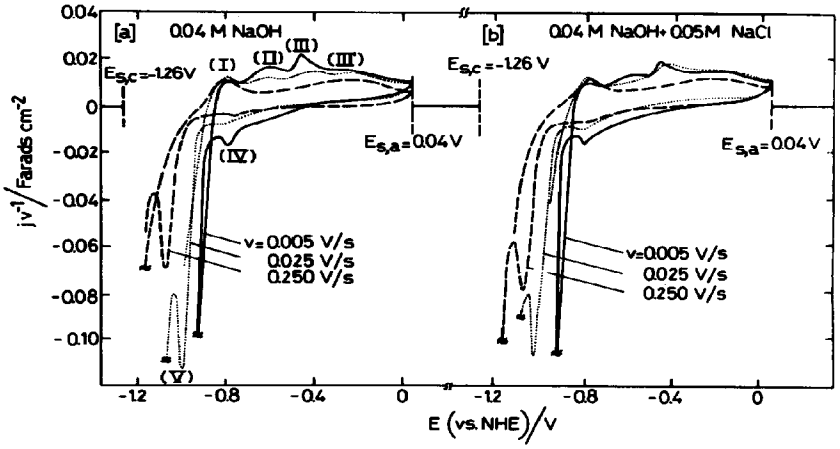

Fig. 1. Single triangular potential sweep (STPS) voltammograms at different v between $E_{s,c} = -1.26$ V and $E_{s,a} = 0.04$ V. (a) 0.04 M NaOH; (b) 0.04 M NaOH + 0.05 M NaCl.

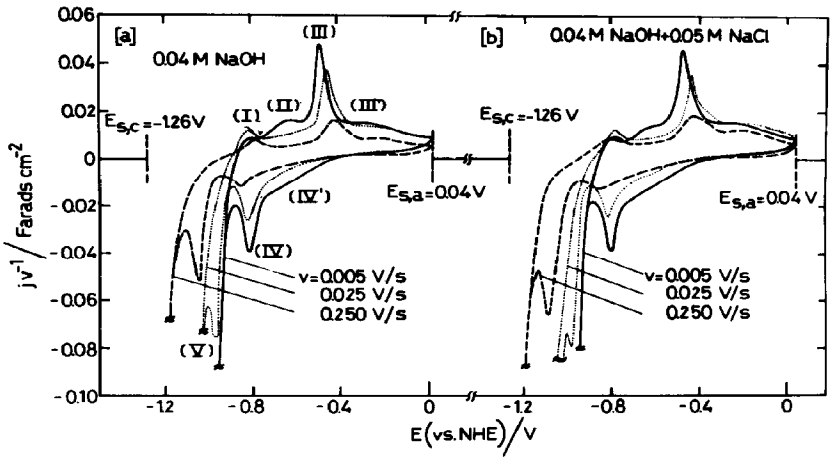

Fig. 2. j/v *vs* potential plots after 10 potential cycles at different v between $E_{s,c} = -1.26$ V and $E_{s,a} = 0.04$ V. (a) 0.04 M NaOH; (b) 0.04 M NaOH + 0.05 M NaCl.

can be noticed (Fig. 2). Conjugated peaks I–II/V are related to the electroformation and electroreduction of the prepassive iron hydroxide layer and the complex conjugated peaks III–III'/IV–IV' have been assigned to the reaction $Fe(II) \rightleftharpoons Fe(III) + e^-$ in the passive film[3]. The voltammetric contours are substantially modified either in going from the first to the tenth sweep at a constant v, or for a constant number of cycles by just changing v. Conversely, only minor voltammetric changes are caused by the presence of NaCl. This can be taken as a preliminary indication that the mechanism of the passive layer formation and its corresponding composition is to a great extent determined by the local concentration of OH^- ions.

Ellipsometric data in 0.04 M NaOH

The transient ellipsometric response resulting under procedure A for iron in 0.04 M NaOH solution ($E_{s,c} = -1.26$; -0.2 V $\leqslant E_{s,a} \leqslant 0.65$ V; and $2 \leqslant \tau \leqslant 5$ s) (Fig. 3) shows an initial fast decrease of δP, to attain a nearly constant value after about 2 s. This result agrees with earlier data obtained from extinction measurements under open circuit conditions[3]. After the anodic oxide formation during the time τ the δP *vs* time plot shows a large linear increasing portion and at the end a limiting value of δP different from the initial one. This means that electroreduction products remain on the metal surface even at relatively high negative potentials (Fig. 3a). The change in δP under a potential holding is accompanied by a definite change in current. Thus, for the anodic potential step a monotonic anodic current decrease can be observed, whereas for the cathodic step at short times a cathodic hump superposed to the base current associated with the HER can be noticed (Fig. 3b). For a constant τ the charge density estimated from the cathodic hump, Q_c, after correction for the e.d.l. charging and HER contributions, increases reasonably linearly with $E_{s,a}$ (Fig. 4). From this plot it results that $Q_c \to 0$ for $(E_{s,a})_{Q_c=0} \simeq -0.68$ V.

Similar runs made including the current switching off during $\tau_0 = 4$ min (procedure B) for an oxide layer

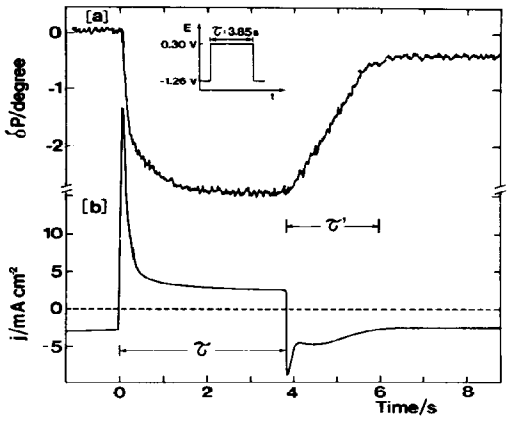

Fig. 3. Dynamic ellipsometric (a) and current transient (b) responses in 0.04 M NaOH during a potential step from $E_{s,c} = -1.26$ V to $E_{s,a} = 0.30$ V including a holding time $\tau = 3.85$ s at $E_{s,a}$.

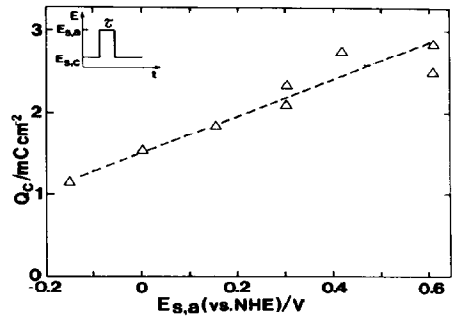

Fig. 4. Dependence of anodic potential holding at $E_{s,a}$ for 3.85 s on the charge Q_c of the cathodic jump superposed to the hydrogen evolution reaction baseline at $E_{s,c} = -1.26$ V in 0.04 M NaOH.

electroformed at 0.61 V (Fig. 5) show that the potential firstly decays to a minimum value of about −0.81 V after about 40 s, and later gradually increases approching a value close to −0.69 V after 4 min. By switching off the current (Fig. 6) δP slightly increases for a few seconds, and finally reaches a constant value substantially lower than the initial one. Afterwards, the following cathodic potential step reproduces the behaviour already described for Figs 1, 3 and 4. This effect which becomes more remarkable by increasing the number of successive runs, can be taken as a first indication that products remaining on the electrode

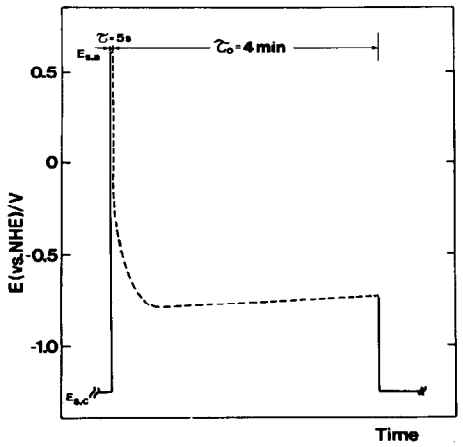

Fig. 5. Open circuit potential evolution after a potential step from $E_{s,c} = -1.26$ V to $E_{s,a} = 0.61$ V including a 5 s holding time at $E_{s,a}$ in 0.04 M NaOH.

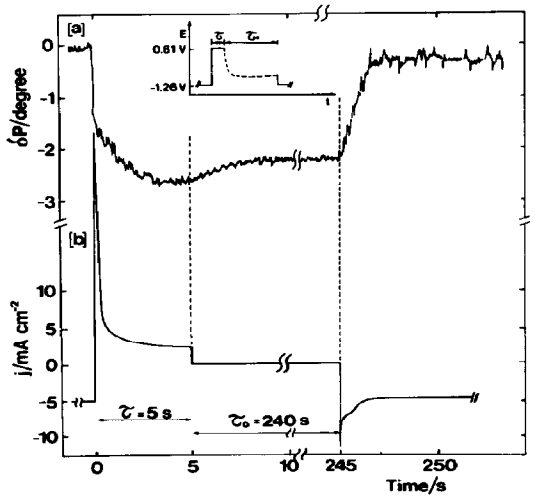

Fig. 6. Dynamic ellipsometric data (a) and current transient (b) in 0.04 M NaOH during a potential programme which includes a potential step at $E_{s,a} = 0.61$ V during $\tau = 5$ s, open circuit during $\tau_0 = 4$ min, and potential stepped to $E_{s,c} = 1.26$ V as indicated in the figure.

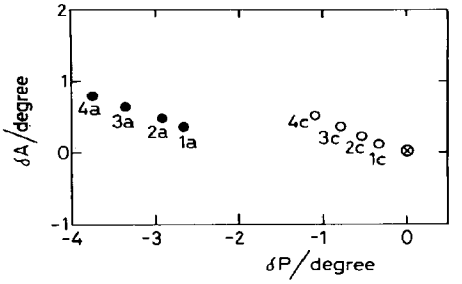

Fig. 7. *P vs A* plot for the surface film at $E_{s,a} = 0$ V (full symbols) and $E_{s,c} = -1.26$ V (open symbols) from the 1st to the 4th potential scans at $v = 20$ V s^{-1} in 0.04 M NaOH.(⊗) identifies freshly electroreduced iron electrode held at $E_{s,c}$ during 10 min.

surface after electroreduction presumably undergo changes in both composition and structure. The plot of ellipsometric data (Fig. 7) shows a clear difference between the behaviour of the layer held at either 0 or −1.26 V. Likewise, during the successive runs for particular values of $E_{s,a}$ and $E_{s,c}$ the ellipsometric data shifts in the same direction. These results suggest that the oxide layer remaining on the surface at high negative potentials progressively accumulates during cycling and its presence has little influence on the subsequent electrooxidation of the base metal in the following anodic potential step. It should be observed that the scattering of ellipsometric data is lower than 10%.

Ellipsometric data in 0.04 M NaOH *containing* NaCl

For $E_{s,a}$ values exceeding the critical pitting potential of iron in base solutions containing NaCl (Fig. 8)[12, 16] the dynamic behaviour of δP and j is at first sight different from that depicted in Fig. 6, and it depends whether the run is made under anodic potential step or open circuit conditions. In the first case a sharp initial decrease in δP and also in j after the e.d.l. charging, comparable to that already observed in the absence of Cl^- ions can be noticed, whereas τ increases δP_{app} and j also increase due to pitting caused by chloride ions. These effects become more remarkable during successive potential steps. Otherwise, for the cathodic potential step initially the situation is comparable to that shown in Fig. 6, but as the number of successive potential steps increases, the contribution of pitting becomes more relevant. Under open circuit conditions a steady pitting corrosion operates which reflects through the constancy of δP and j values. Hence, for a preset potential step it is reasonable to expect that both δP and Q_c change linearly with the potential of anodic step (Fig. 9). The extrapolation of δP *vs* $E_{s,a}$ (Fig. 9a) and Q_c *vs* $E_{s,a}$ (Fig. 9b), at $\delta P \to 0$ and $Q_c \to 0$ yield $E^0_{\delta P} = -0.73$ V and $E^0_{Q_c} = -0.66$ V, respectively. On the other hand, the change of P at high negative potentials (ΔP_c) measured after the anodic potential step (Fig. 10) also fits a linear ΔP_c *vs* $E_{s,a}$ relationship, whose extrapolation to $\Delta P_c \to 0$ approaches $E^0_{\Delta P_c} \simeq -0.55$ V. Obviously, the reproducibility of results in the NaCl solutions is lower than in NaCl free base due to pitting corrosion.

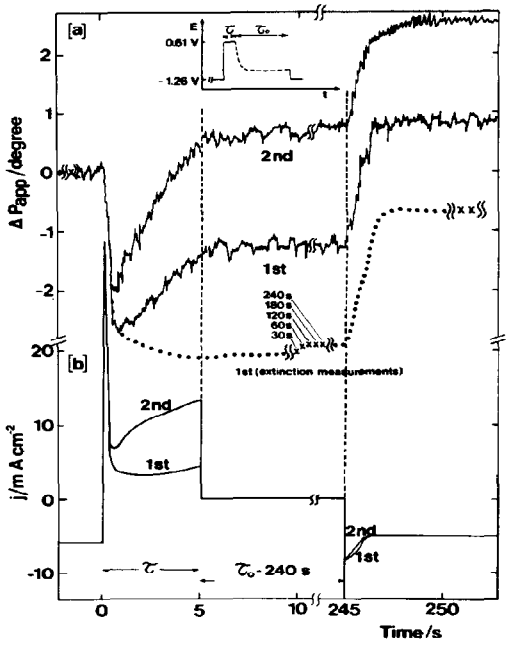

Fig. 8. Dynamic ellipsometric measurements (a) and current transient (b) in 0.04 M NaOH + 0.05 M NaCl. Each cycle of the potential programme as indicated in figure.

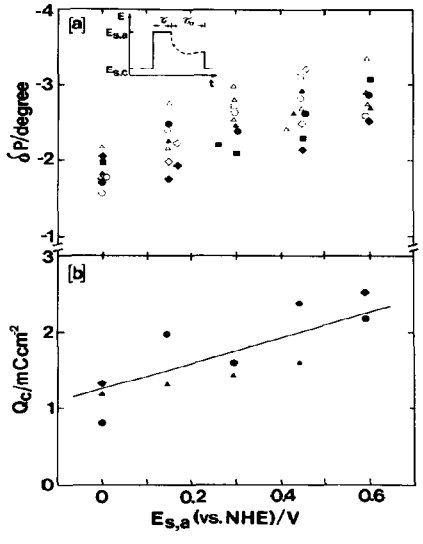

Fig. 9. (a) Comparison between the dependences of $E_{s,a}$ on the dynamic ellipsometric (open symbols) and extinction measurements (full symbols) data. The potential programme consists of a potential step at different $E_{s,a}$ during 2 s, open circuit during 4 min, and potential stepped to $E_{s,c} = -1.26$ V. (b) Dependence of $E_{s,a}$ on the properly corrected Q_c at $E_{s,c}$. (△, ▲) 0.04 M NaOH; (◇, ◆) 0.04 M NaOH + 0.01 M NaCl; (○, ●) 0.04 M NaOH + 0.05 M NaCl; (□, ■) 0.04 M NaOH + 0.3 M NaCl.

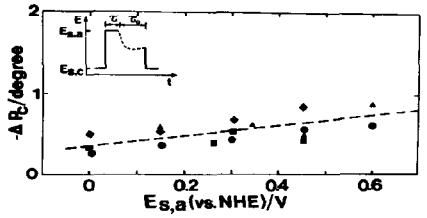

Fig. 10. Dependence of the anodic potential step value on the variation of P measured at $E_{s,c} = -1.26$ V after the potential programme indicated in Fig. 9. (▲) 0.04 M NaOH; (◆) 0.04 M NaOH + 0.01 M NaCl; (●) 0.04 M NaOH + 0.05 M NaCl; (■) 0.04 M NaOH + 0.3 M NaCl.

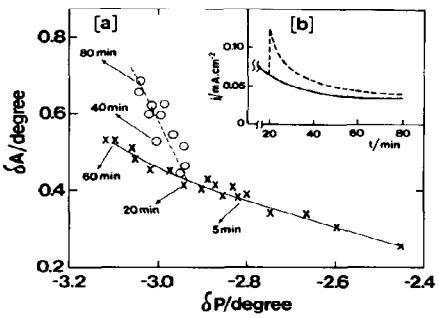

Fig. 11. Comparative P vs A plots (a) and current transient (b) in NaCl free [full lines, (x)] and NaCl added solutions [dashed lines, (o)] in 0.04 M NaOH solutions during the potential holding at 0.03 V after a potential scan at $v = 20$ V s^{-1} from $E_{s,c} = -1.36$ V. The NaCl addition up to 0.05 M was made after 20 min holding time at $E_{s,a} = 0.03$ V.

The time variation of the ellipsometric parameters by holding a constant applied potential depends strongly on the presence of NaCl in solution. This is clearly seen by adding NaCl up to 0.05 M in 0.04 M NaOH after the ellipsometric readings at $E_{s,a} = 0.03$ V (Fig. 11). The separation of the corresponding δA vs $E_{s,a}$ and δP vs $E_{s,a}$ plots in the absence and in the presence of added NaCl increases with time (Fig. 11a). On the other hand, after the incorporation of NaCl the current transient increases as compared to that recorded in plain base solution (Fig. 11b).

DISCUSSION

Electrochemical and ellipsometric data show that the growth of the passive film on iron in alkaline solution in the absence of NaCl involves two distinguishable stages and correspondingly, the formation of two juxtaposed layers[3, 17–20]. According to the present results the inner layer (barrier layer) in contact with the metal surfaces is firstly formed, at a relatively low rate, as derived from current transients and first voltammetric cycles, the latter being characterized by the prevalence of peaks I and II. Conversely, the outer layer although subsequently formed, exhibits a relatively large growth rate. Thus, the contribution of

peak III related to the formation of a hydrous porous Fe(III)-oxide structure becomes increasingly important with the number of voltammetric cycles. Both the increase in the anodic polarization and cathodic electroreduction time promote the progressive increase of the outer layer charge. The present results also confirm that during the voltammetric cycles (Fig. 2) the partial electroreduction of the inner layer can be accomplished. This is in agreement with the fact that the extrapolation of the δP *vs* $E_{s.a}$ plot to $\delta P \to 0$, occurs for a value of E slightly more positive than that of the voltammetric peak I related to $Fe(OH)_2$ monolayer formation. As a matter of fact, the complete electroreduction of the barrier layer takes place rather slowly in the potential range of peak V[3, 11]. Otherwise, the barrier layer can be regenerated already after 1.5–2.0 s after the anodic potential step has been applied. On the other hand, the outer layer should imply a hydrous structure with a large initial content of Fe(III) species, which in turn are able to participate in relatively fast redox processes[3]. It should be noticed that recent voltammetric data obtained with iron hydroxide layers precipitated on platinum electrodes are in agreement with these conclusions[21, 22].

The precedent description of iron passivation in base solution can be useful to interpret the influence of NaCl in the entire reaction. Thus, it appears that the presence of NaCl at least in the concentration range covered by this work, remains unnoticed in the time range associated with the formation of the barrier layer. A different situation arises in the time range related to the growth of the outer layer coupled to pitting corrosion, the latter becoming noticeable only after the barrier layer has been near completely formed.

The reaction yielding the initial thin $Fe(OH)_2$ layer is determined by the high adsorbability of OH^- ions and can be written as follows[21, 23, 24]:

$$Fe + 2(OH^-) = [Fe(OH)_2]_I + 2e^-, \qquad (1)$$

which later transforms into a Fe_3O_4 layer (barrier layer) as the potential increases. The complex nature of the overall reaction (1) was discussed in detail in previous publications[23, 24].

The growth of the outer layer (II) implies the formation of Fe(III) species under the form of a hydrous Fe(III) oxy-hydroxide layer. The corresponding reaction occurs through the electro-oxidation of $Fe(OH)_2$ which is immediately replenished. The overall process can be expressed in a simple way by the series of reactions:

$$Fe + 3(OH^-) \overset{-(2e^-)}{\rightleftharpoons} [Fe(OH)_2]_I + OH^- \overset{-(e^-)}{\rightleftharpoons} [Fe(OH)_3]_{II}, \qquad (2)$$

where the brackets denote hydrous species.

Finally, pitting corrosion requires a competitive interaction between Cl^- and OH^- ions with layers I and II and the proper iron surface. This can be written as follows:

$$2[Fe(OH)_2]_I + 3Cl^- = [FeCl_3]_I + [Fe(OH)_2]_I + 2OH^- + e^-, \qquad (3a)$$

$$[FeCl_3]_I + 3OH^- = [Fe(OH)_3]_{II} + 3Cl^-. \qquad (3b)$$

Therefore, the presence of Cl^- ion can promote the increase of the outer layer charge, and in this case, the induction time for pitting can be related to the adsorption of Cl^- ion. The outer layer, whose thickness increases during potential cycling[3, 13], consists of either a very porous film containing a considerable amount of electrolyte or a film of electrolyte containing partially dissolved reaction products. Reaction (3a) can be, in principle, supported by recent measurements employing radiotracer techniques, in borate buffer, which indicate adsorption and absorption of chloride ions on passive iron[25]. The time constant for the chloride adsorption is about 1 min, while that related to the chloride absorption into the passive layer is in the order of 60 min. The latter process is controlled by diffusion and it increases linearly with potential. However, in contrast to these conclusions comparable studies made by Auger electrospectroscopy and X-ray photoelectron spectroscopy[26] were unable to detect Cl^- ion incorporation into the oxide film. In addition it should be mentioned that in these optical studies no film thinning caused by Cl^- ion could be observed, a fact which seems to occur as reported in an earlier work[27].

As discussed in early work[3] during the voltammetric cycling the following reversible reaction:

$$e^- + [Fe(III)]\,(\text{layer II}) = [Fe(II)]\,(\text{layer II}), \qquad (4)$$

takes place at the outer layer, so that the various processes above described can be summarized in the following reaction scheme:

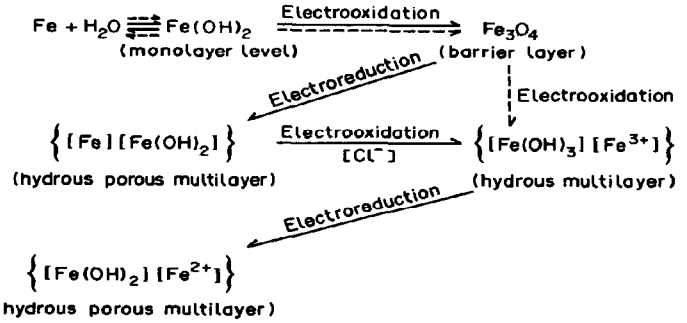

Full arrows indicate the reaction pathway under potential cycling conditions, while dashed arrows show the electro-oxidation process during an anodic

potential step. At large potential holding times in the passive region, the [$Fe(OH)_3$] hydrous species (layer II) tends to a [FeOOH] layer. Similarly, the inner portion of the outer layer II after prolonged potential cycling can be considered also as constituted mainly by [FeOOH] species.

According to these reactions the relative amount of layers I and II should be remarkably dependent on the presence of Cl^- ion, on the type and characteristics of the potential program, namely triangular sweep or potential step and on the cation in solution, since the incorporation of the latter in the complex layer should alter its water content and ionic composition. This is apparently the case of Ca^{2+} ions as compared to Na^{2+} in the passivation of iron in base solutions as concluded from previous work[3].

Acknowledgements—This work was financially supported by the Consejo Nacional de Investigaciones Científicas y Técnicas and the Comisión de Investigaciones Científicas de la Provincia de Buenos Aires. This work was partially supported by the Regional Program for the scientific and technological development of the Organization of the American States.

REFERENCES

1. G. Nazri, E. Yeager and B. D. Cahan, Tech. Rep. No. 1, Proj. NR SRO-009/7-30-79, Case Western Reserve University, Cleveland (1981).
2. K. E. Heusler, In *Encyclopedia of Electrochemistry of the Elements* (Edited by A. J. Bard), Vol. 9A, pp. 229–381, Marcel Dekker, New York (1982).
3. O. A. Albani, J. O. Zerbino, J. R. Vilche and A. J. Arvia, *Electrochim. Acta* **31,** 1403 (1986).
4. M. Froelicher, A. Hugot-Le Goff, C. Pallotta, R. Dupeyrat and M. Mason, in *Passivity of Metals and Semiconductors* (Edited by M. Froment), pp. 101–105 Elsevier, Amsterdam, (1983).
5. J. Dünnwald, R. Losy and A. Otto, In *Passivity of Metals and Semiconductors* (Edited by M. Froment), pp. 107–112 Elsevier, Amsterdam, (1983).
6. J. Dünnwald and A. Otto, *Z. Anal. Chem.* **319,** 738 (1984).
7. Z. Q. Huang and J. L. Ord, *J. electrochem. Soc.* **132,** 24 (1985).
8. T. Zakroczymski, C. J. Fan and Z. Szklarska-Smialowska, *J. electrochem. Soc.* **132,** 2862 (1985).
9. S. Haupt, C. Calinski, U. Collisi, H. W. Hoppe, H. D. Speckmann and H. H. Strehblow, *Surf. Interface Anal.* **9,** 357 (1986).
10. C. Gutiérrez and M. A. Martínez, *J. electrochem. Soc.* **133,** 1873 (1986).
11. S. Juanto, J. O. Zerbino, J. R. Vilche and A. J. Arvia, In *Surfaces, Inhibition, and Passivation* (Edited by E. McCafferty and R. J. Brodd), pp. 226–238 The Electrochemical Society, Pennington, (1986).
12. T. Zakroczymski, C. J. Fan and Z. Szklarska-Smialowska, *J. Electrochem. Soc.* **132,** 2868 (1985).
13. M. G. Alvarez and J. R. Galvele, *Corros. Sci.* **24,** 27 (1984).
14. N. Sato and K. Kudo, *Electrochim. Acta* **16,** 447 (1971).
15. N. Sato, *Boshoku Gijutsu* **23,** 535 (1974).
16. O. A. Albani and J. R. Vilche, in preparation.
17. J. R. Vilche and A. J. Arvia, Proc. 7th Intern. Congr. Met. Corros., Rio de Janeiro, pp. 245–256 (1978).
18. R. S. Schrebler Guzmán, J. R. Vilche and A. J. Arvia, *Electrochim. Acta* **24,** 395 (1979).
19. V. A. Macagno, J. R. Vilche and A. J. Arvia, *J. Appl. Electrochem.* **11,** 417 (1981).
20. R. S. Schrebler Guzmán, J. R. Vilche and A. J. Arvia, *J. Appl. Electrochem.* **11,** 551 (1981).
21. M. E. Vela, J. R. Vilche and A. J. Arvia, in *Passivity of Metals and Semiconductors* (Edited by M. Froment), pp. 59–65 Elsevier, Amsterdam, (1983).
22. M. E. Vela, J. R. Vilche and A. J. Arvia, *Electrochim. Acta* **31,** 1633 (1986).
23. J. O. Zerbino, J. R. Vilche and A. J. Arvia, *J. Appl. Electrochem.* **11,** 703 (1981).
24. M. E. Vela, J. R. Vilche and A. J. Arvia, *J. Appl. Electrochem.* **16,** 490 (1986).
25. V. Jovancicevic, J. O'M. Bockris, J. L. Carbajal, P. Zelenay and T. Mizuno, *J. electrochem. Soc.* **133,** 2219 (1986).
26. R. Goetz, B. MacDougall and M. J. Graham, *Electrochim. Acta* **31,** 1299 (1986).
27. M. Janik-Czachor and S. Kaszczyszyn, *Werkstoffe u. Korros.* **33,** 500 (1982).